

# Optical recombination lines

$$(9.4.2) \alpha_v \ll 1$$

Balmer lines observed in optical

Only need know # of particles in  $n_j$  to use eq 9.8  
(expression for  $j_v$ )

$$\Rightarrow \dots \Rightarrow \int_v j_v dv = \frac{1}{4\pi} h \nu_{ji} \alpha_{ji} n_e n_i \approx \frac{1}{4\pi} h \nu_{ji} \alpha_{ji} n_e^2$$

we 6.17 with 9.13

freq of line  $\nu_{ji}$

$\alpha_{ji}$  effective recombination coeff see table 9.4

$n_e$  electron density

$n_i$  density

$\propto$  density

Set to equal

$$\Rightarrow \dots \Rightarrow \int_v I_v dv = \frac{1}{4\pi} h \nu_{ji} \alpha_{ji} n_e^2 l = 2.66 \times 10^{17} h \nu_{ji} \alpha_{ji} EM$$

Intensity over the line

$\propto$  temp  $\left[ \frac{pe}{an^6} \right]$



**Table 9.4.** Effective recombination coefficients<sup>a</sup>

$\alpha_{j,i} \text{ (cm}^3 \text{ s}^{-1}\text{)}$	Temperature (K)		
	5 000	10 000	20 000
$\alpha_{3,2} \text{ (H}\alpha\text{)}$	$2.21 \times 10^{-13}$	$1.17 \times 10^{-13}$	$5.97 \times 10^{-14}$
$\alpha_{4,2} \text{ (H}\beta\text{)}$	$5.41 \times 10^{-14}$	$3.03 \times 10^{-14}$	$1.61 \times 10^{-14}$

<sup>a</sup>Case B recombination has been assumed (see Sect. 9.4.2). H $\alpha$  values are from Ref. [160] and H $\beta$  values are from Ref. [115]. For the latter reference, means for the densities,  $10^2$  and  $10^4 \text{ cm}^{-3}$  are given.

↑ well known, for any 2 lines in an atom,

$E_M$  is the same

$$\frac{\int \underline{I}_\nu d\nu \text{ (j} \rightarrow \text{i)}}{\int \underline{I}_\nu d\nu \text{ (k} \rightarrow \text{m)}}$$

$$= \frac{\nu_{ji} \alpha_{ji}}{\nu_{km} \alpha_{km}}$$

$\propto \text{Temp}$

Ex H $\alpha$  & H $\beta$

Assume HII region  
T =  $10^4 \text{ K}$

$$\frac{\nu_{32} \alpha_{32}}{\nu_{4-2} \alpha_{42}}$$

$$= \left[ \begin{array}{l} \text{table C.1} \\ \text{table 9.4} \end{array} \right]$$

$$= \frac{486.132}{656.288} \cdot \frac{1.17 \cdot 10^{-13}}{3.03 \cdot 10^{-14}} = 2.86$$



line ratio =  
diagnostic to  
get temperature  
for HII clouds etc

Table 9.5. Sample line ratios for the hydrogen balmer series<sup>a</sup>

Line ratio	T <sub>e</sub> (K)					
	5000		10000		20000	
	n <sub>e</sub> (cm <sup>-3</sup> )		n <sub>e</sub> (cm <sup>-3</sup> )		n <sub>e</sub> (cm <sup>-3</sup> )	
	10 <sup>2</sup>	10 <sup>4</sup>	10 <sup>2</sup>	10 <sup>4</sup>	10 <sup>2</sup>	10 <sup>4</sup>
H $\alpha$ /H $\beta$	3.04	3.00	2.86	2.85	2.75	2.74
H $\gamma$ /H $\beta$	0.458	0.460	0.468	0.469	0.475	0.476
H $\delta$ /H $\beta$	0.251	0.253	0.259	0.260	0.264	0.264
H $\epsilon$ /H $\beta$	0.154	0.155	0.159	0.159	0.162	0.163

<sup>a</sup>Ref. [50]. Case B recombination has been assumed (see Sect. 9.4.2).

can form the  
ratio of any two lines that we observe  
(result not dependent on broadening effects)

once we have T<sub>e</sub>  $\Rightarrow$  find density (knowing D)

(via eq 9.14)

But a few complications

case A : all lines opt thin

case B : Lyman lines (UV) which are optically thick

$\Rightarrow$  affects the line ratios  $\sim 3\%$

ratio  
weakly  
dependent  
on T

for  
Balmer  
lines!

only changes  
a few %



Use other line ratios! pick lines optically thin  
and with stronger temp dependencies

$[OIII]$  &  $[NII]$  — square brackets = forbidden lines

5007

“nebulium” — could not be  
seen in Earth lab  
— too high density



$$R_O = \frac{I(\lambda 4959) + I(\lambda 5007)}{I(\lambda 4363)} = \frac{7.73 \exp[(3.29 \times 10^4)/T_e]}{1 + 4.5 \times 10^{-4} [n_e/(T_e)^{1/2}]} \quad ([OIII]) \quad (9.17)$$

$$R_N = \frac{I(\lambda 6548) + I(\lambda 6583)}{I(\lambda 5775)} = \frac{6.91 \exp[(2.50 \times 10^4)/T_e]}{1 + 2.5 \times 10^{-3} [n_e/(T_e)^{1/2}]} \quad ([NII]) \quad (9.18)$$

these ratios most sensitive to temp

choose your lines carefully

optical affected by dust - extinction - reddening

- pick lines close to each other

- can also correct for extinction with  
eg. Balmer line ratios.



↓ RRLs

# Radio recombination lines

highest quantum #  
transitions:  $n \geq 40$

at high  $n$ , transitions  
close together

⇒ radio  $\lambda$   
redshift

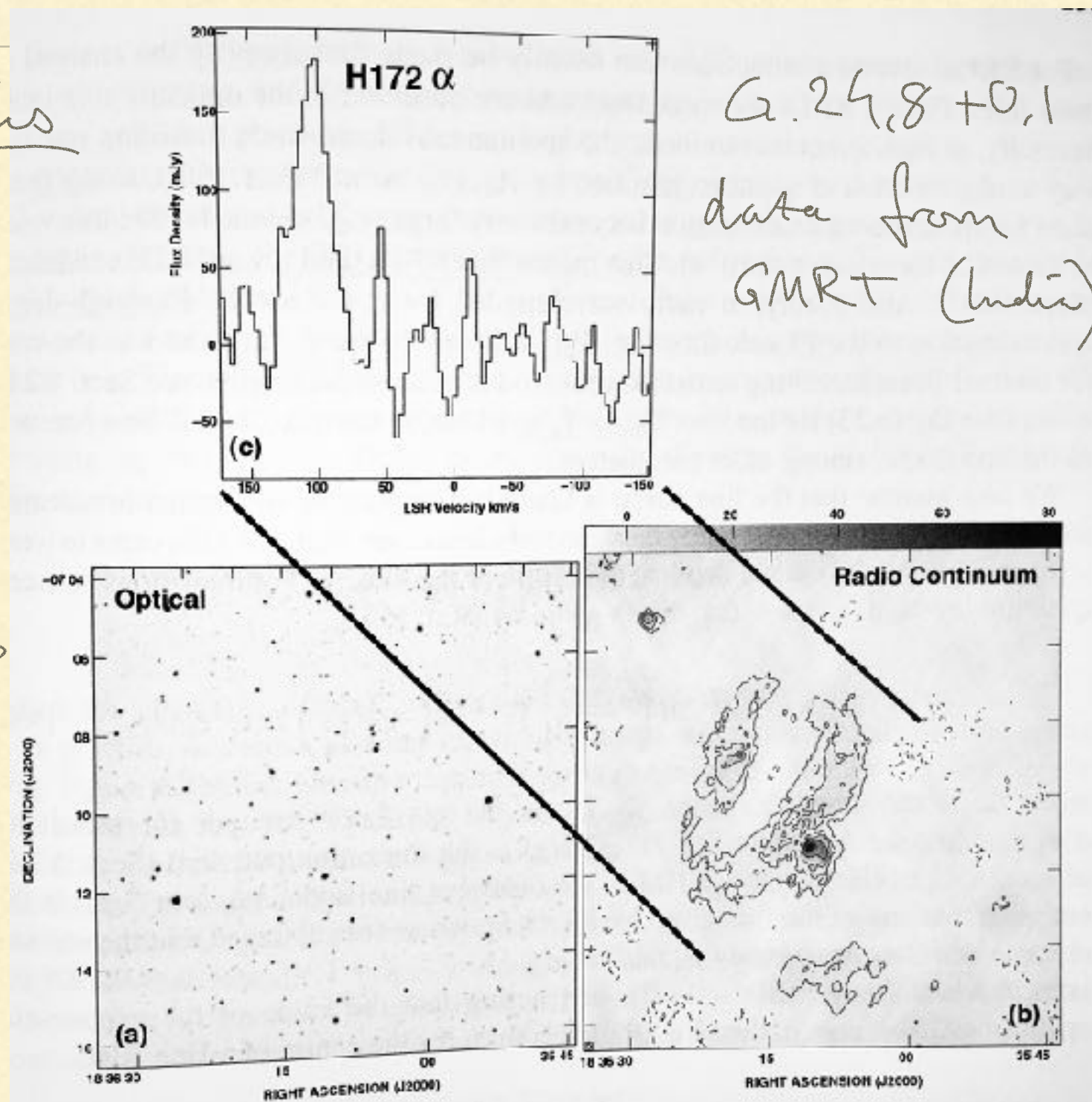
& low probability  
for these transitions.

⇒ RRLs weak  
many transitions

$n = 766$  Carbon  $\nu = 14 \text{ MHz}$

for H  $n = 1600$  theorized to be possible

radio not obscured by dust ⇒ RRLs only way to see some  
regions



G.24.8+0.1  
data from  
GMRT (India)

Fig 9.6



DIG Diffuse ionized gas of MW

lines  $\Rightarrow$  doppler  $\Rightarrow$  distances  
(cannot be done with continuum)

Simplifications promised:  $\begin{cases} \tau_v \ll 1 \\ \text{LTE conditions} \\ h\nu \ll kT \Rightarrow \text{R-J} \end{cases}$

optically thin:  $\{T_{\text{exp}} \& \text{density}\} \quad T_B = T_e \tau_v$

Observe RRL, — superimposed on the  
continuum radiation — Bremsstrahlung in  
radio region

$\Rightarrow \tau$  &  $T_B$  (eq 8.12 & 8.13)



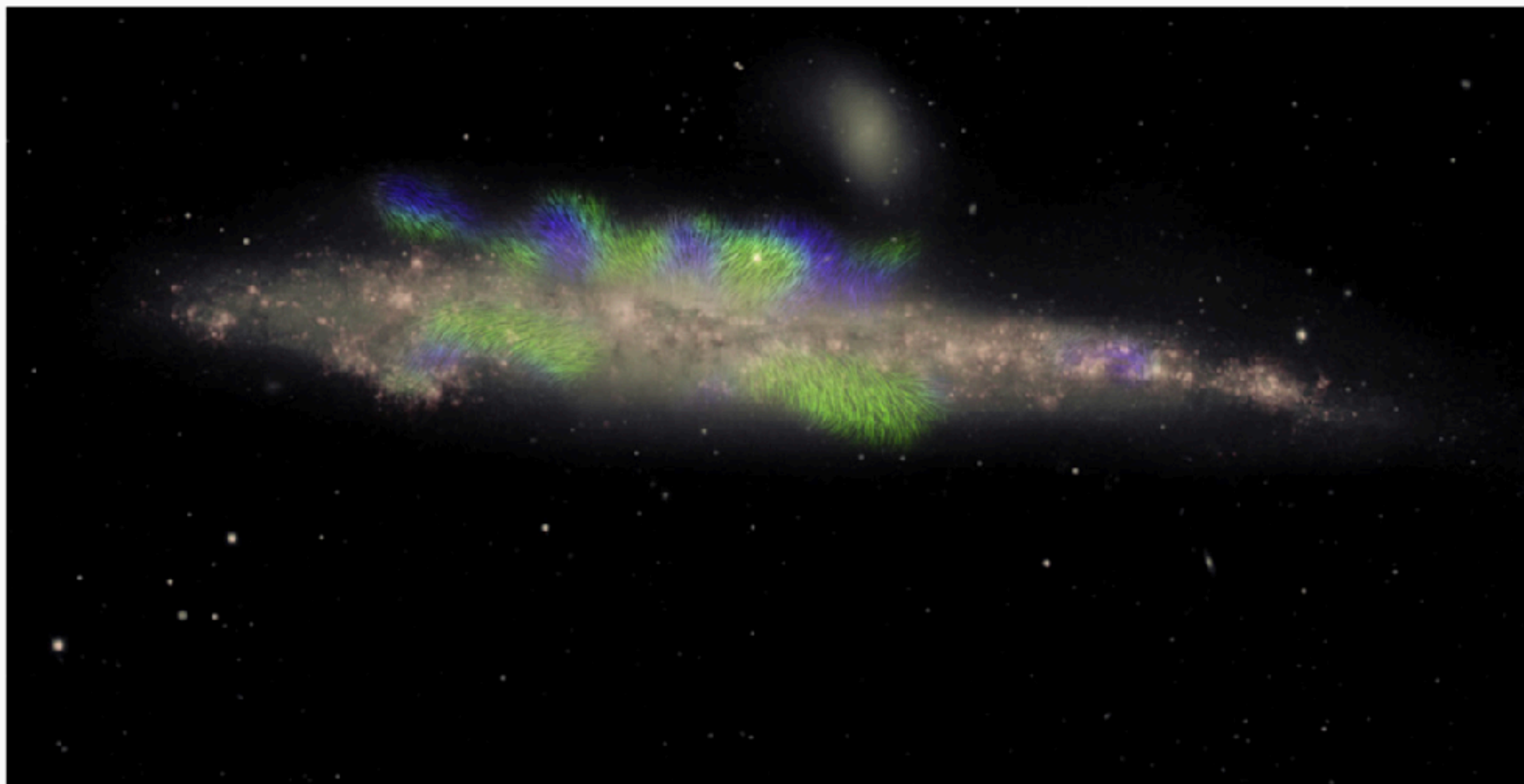


Home > News > News Release: November 26, 2019 at 8:00 am EST

<https://public.nrao.edu/news/giant-magnetic-ropes/>

 Print  PDF

## IMAGE RELEASE: Giant Magnetic Ropes in a Galaxy's Halo



*Credit: Composite image by Jayanne English of the University of Manitoba, with NRAO VLA radio data from Silvia Carolina Mora-Partiarroyo and Marita Krause of the Max-Planck Institute for Radioastronomy. The observations are part of the project Continuum HALos in Nearby Galaxies – an EVLA Survey (CHANG-ES). The optical data were from the Mayall 4-meter telescope, collected by Maria Patterson and Rene Walterbos of New Mexico State University. Arpad Miskolczi of the University of Bochum provided the software code for tracing the magnetic field lines.*





## Astrophysics &gt; Astrophysics of Galaxies

**CHANG-ES XV: Large-scale magnetic field reversals in the radio halo of NGC 4631**

Silvia Carolina Mora-Partiarroyo, Marita Krause, Aritra Basu, Rainer Beck, Theresa Wiegert, Judith Irwin, Richard Henriksen, Yelena Stein, Carlos J. Vargas, Volker Heesen, Rene A. M. Walterbos, Richard J. Rand, George Heald, Jiangtao Li, Patrick Kamienieski, Jayanne English

(Submitted on 16 Oct 2019)

NGC 4631 is an interacting galaxy which exhibits one of the largest gaseous halos observed among edge-on galaxies. We aim to examine the synchrotron and polarization properties of its disk and halo emission with new radio continuum data. Radio continuum observations of NGC 4631 were performed with the Karl G. Jansky Very Large Array at C-band (5.99 GHz) in the C & D array configurations, and at L-band (1.57 GHz) in the B, C, & D array configurations. The Rotation Measure Synthesis algorithm was utilized to derive the polarization properties.

We detected linearly polarized emission at C-band and L-band. The magnetic field in the halo is characterized by strong vertical components above and below the central region of the galaxy. The magnetic field in the disk is only clearly seen in the eastern side of NGC 4631, where it is parallel to the plane of the major axis of the galaxy. We detected for the first time a large-scale, smooth Faraday depth pattern in a halo of an external spiral galaxy, which implies the existence of a regular (coherent) magnetic field.

A quasi-periodic pattern in Faraday depth with field reversals was found in the northern halo of the galaxy. The field reversals in the northern halo of NGC 4631, together with the observed polarization angles, indicate giant magnetic ropes (GMRs) with alternating directions. To our knowledge, this is the first time such reversals are observed in an external galaxy.

Comments: 8 pages, 7 figures, accepted to be published in A&A

Subjects: Astrophysics of Galaxies (astro-ph.GA)

Cite as: arXiv:1910.07590 [astro-ph.GA]

(or arXiv:1910.07590v1 [astro-ph.GA] for this version)

**Bibliographic data**

[Enable Bibex(What is Bibex?)]

**Submission history**

From: Yelena Stein [view email]

[v1] Wed, 16 Oct 2019 19:58:15 UTC (3,357 KB)

*Which authors of this paper are endorsers?* | Disable MathJax (What is MathJax?)